Journal of Molecular Structure 1252 (2022) 132053

Contents lists available at ScienceDirect

Journal of Molecular Structure

journal homepage: www.elsevier.com/locate/molstr

Rotationally resolved electronic spectroscopy of 6-methylindole: Structures, transition moments, and permanent dipole moments of ground and excited singlet states

Marie-Luise Hebestreit[a,*], Hajo Böschen[a], Hilda Lartian[a], W. Leo Meerts[b], Michael Schmitt[a]

[a] Heinrich-Heine-Universität, Institut für Physikalische Chemie I, Düsseldorf D-40225, Germany
[b] Radboud University, Institute for Molecules and Materials, Felix Laboratory, Toernooiveld 7c, Nijmegen 6525 ED, The Netherlands

ARTICLE INFO

Article history:
Received 19 August 2021
Revised 24 November 2021
Accepted 27 November 2021
Available online 6 December 2021

Keywords:
Methylindole
Excited state
Electronic structure
L_a-state
L_b-state

ABSTRACT

The rotationally resolved electronic spectrum of the $S_1 \leftarrow S_0$ electronic origin band of 6-methylindole (6-MI) has been measured in a molecular beam and has been fit to rigid asymmetric rotor Hamiltonians in both electronic states using evolutionary strategies. Rotational constants, dipole moments in both electronic states, and orientation of the transition dipole moment in the inertial frame of the molecule have been determined and compared to the results of *ab initio* calculations. Both the values of the permanent dipole moments as of the transition dipole moment point to an L_b-state as lowest electronically excited state in 6-MI.

1. Introduction

The position of electronically excited states of substituted indoles critically depends on the electronic nature of the substituent and on the position of substitution. On the other hand, the position of the substituent in the chromophore also influences the properties of the substituents. In indole and substituted indoles, three low-lying electronically excited singlet states are involved in the photophysics and photochemistry of these compounds. These states can clearly be distinguished by their spectral fingerprints. The lowest two excited singlet states arise from $\pi\pi^*$ excitations and are classified according to the labeling of Platt [1], later extended by Weber [2] as ^1L_a and ^1L_b states [3]. Their energetic order depends on the electronic nature and on the position of the substituent. While in indole [4–7] and in most substituted indoles [8–14] the lowest excited singlet state has L_b-character, a few exceptions are found, in which the L_a-state is the lowest excited singlet state [12,13,15–17]. These two states can easily be distinguished by the orientation of the transition dipole moment, which points for L_b-states away from the pyrrolic NH group, and by their permanent dipole moment, which is higher for L_a- than for L_b-states. A third low-lying excited singlet state has been identified by Sobolewski and Domcke [18] as $\pi\sigma^*$ state, which is repulsive along the NH coordinate of the pyrrole moiety and is determined by a σ^* Rydberg-type orbital centered at the NH group.

Here, we present a study 6-methylindole (6-MI), in which a methyl group is attached to position 6 of the benzene ring in indole. In the group of Meerts, 3-, and 5-MI have been studied using rotationally resolved electronic spectroscopy of the ^1L_b origin [19]. Korter and Pratt examined 1-, 3-, and 5-MI and their van der Waals bound argon clusters and determined the barriers to internal rotation of the methyl group in the ground and lowest excited singlet states [20]. The torsional spectra of several methylindoles along with an analysis of the barrier heights in the different electronic states was presented by Bickel *et al.* [21].

2. Computational methods

2.1. Quantum chemical calculations

Structure optimizations were performed employing a Dunning's correlation-consistent polarized valence triple zeta (cc-pVTZ) basis set from the TURBOMOLE library [22,23]. The equilibrium geometries of the electronic ground and the lowest excited singlet states were optimized using the approximate coupled cluster singles and doubles model (CC2) employing the resolution-of-the-identity (RI) approximation [24–26]. For the structure optimizations spin-component scaling (SCS) modifications to CC2 were taken into account [27]. Vibrational frequencies and zero-point corrections

* Corresponding author.
E-mail address: marie-luise.hebestreit@hhu.de (M.-L. Hebestreit).

https://doi.org/10.1016/j.molstruc.2021.132053

to the adiabatic excitation energies were obtained from numerical second derivatives using the NumForce script [28].

2.2. Fits of the rovibronic spectra using evolutionary algorithms

Evolutionary algorithms have proven to be perfect instruments for an automated fit of rotationally resolved electronic spectra, even for large molecules and dense spectra [29–32]. They provide to find the global optimum in a multi-parameter optimization. In general evolutionary strategies are inspired by evolutionary processes in nature, including reproduction, mutation and selection. For the analysis of the presented high-resolution spectra we apply the covariance matrix adaptation evolution strategy (CMA-ES), which is described in detail elsewhere [31,33,34].

For the fits the Hamiltonian for a simple asymmetric rotor with Watson's A-reduction is used [32]. For the Stark spectrum additional terms arise and the Stark-Hamiltonian can be factorized into the three projections of the permanent dipole moment onto the main inertial axes with the matrix elements obtained from Gordy and Cook [35].

3. Experimental methods

3.1. Rotationally resolved electronic spectroscopy

6-MI (≥ 98%) was purchased from Fluorochem and used without further purification. The sample was heated to 85 °C and co-expanded with 300 mbar of Argon through a 147 μm nozzle into the vacuum to record rotationally resolved electronic spectra. To form the molecular beam a beam machine consisting of three differentially pumped vacuum chambers with two skimmers, with the diameter of 1 mm and 3 mm, linearly aligned inside the machine is used. The resulting molecular beam was crossed at right angles with the laser beam 360 mm downstream of the nozzle. To create the excitation beam, a single frequency ring dye laser (Sirah Matisse DS) operated with Rhodamine 6G was pumped by 10 W of the 532 nm line of a diode pumped solid state laser (Spectra-Physics Millennia eV). The resulting power of about 5 mW during the experiments was reached by the frequency doubling of the fluorescence light of the dye laser in an external folded ring cavity (Spectra Physics Wavetrain). To collect the fluorescence light of the sample perpendicular to the plane, defined by laser and molecular beam, onto the photocathode of an UV enhanced photomultiplier tube (Thorn Emi 9863QB) a light collecting system consisting of a concave mirror and two planoconvex lenses is used. The signal output was then discriminated and digitized by a photon counter and transmitted to a PC for data recording and processing. A *quasi* confocal Fabry-Perot interferometer was used to determine the relative frequency. The absolut frequency was obtained by comparing the recorded spectrum to the tabulated lines in the iodine absorption spectrum [36]. A detailed description of the experimental setup for rotationally resolved laser induced fluorescence spectroscopy has been given previously [37,38].

3.2. Rotationally resolved electronic Stark spectroscopy

To record rotationally resolved electronic Stark spectra a static electric field is required. The Stark plates consist of a parallel pair of electroformed nickel wire grids (18 mesh per mm, 50 mm diameter) with a transmission of 95 % in the UV and an effective distance of 23.49 ± 0.05 mm, symmetrically aligned with respect to the laser beam. The distance of the grids was calibrated using the accurately known dipole moment of benzonitrile [39,40]. The polarization plane of the incoming laser beam can be rotated by 90° inside the vacuum chamber by means of an achromatic λ/2 plate (Bernhard Halle 240 - 380 nm), which can be pushed in or pulled out of the laser beam using a linear motion vacuum feedthrough. One can choose between a parallel (selection rules $\Delta M = 0$) and perpendicular (selection rules $\Delta M = \pm 1$) set-up by changing the plane of polarization.

4. Results

4.1. Computational results

The SCS-CC2/cc-pVTZ optimized structure of 6-MI yields an inertial defect of -3.12 amu Å^2 in the ground and -3.19 amu Å^2 in the lowest excited singlet state (L_b). The inertial defect of -3.12 amu Å^2 for the S_2 (L_a) state is very similar to the value in the S_1-state. A clear indication for the L_b-state being the lowest excited singlet state are the main contributions to the excitation to the lowest excited singlet state at the SCS-CC2 level of theory: 56.5 % LUMO ← HOMO-1 + 22.4 % LUMO+1 ← HOMO + 10.9 % LUMO ← HOMO and 4.1 % LUMO+1 ← HOMO-1, while the second excited singlet state is a nearly pure LUMO ← HOMO excitation (Fig. 1).

The molecular parameters (rotational constants *A*, *B*, and *C* in both electronic states, the inertial defects ΔI, the angle θ of the transition dipole moment with the inertial *a*-axis, the angle θ_D of the permanent dipole moment with the inertial *a*-axis, and the zero-point corrected origin frequency ν_0) of the ground and both electronically excited states are compiled in Table 1 and are compared to the experimental results, which are described in detail in Section 4.2.

The calculated angle θ of the transition dipole moment (TDM) for excitation to the lowest excited singlet state is +16.1° ° with respect to the inertial *a*-axis, what is another indication for the L_b-

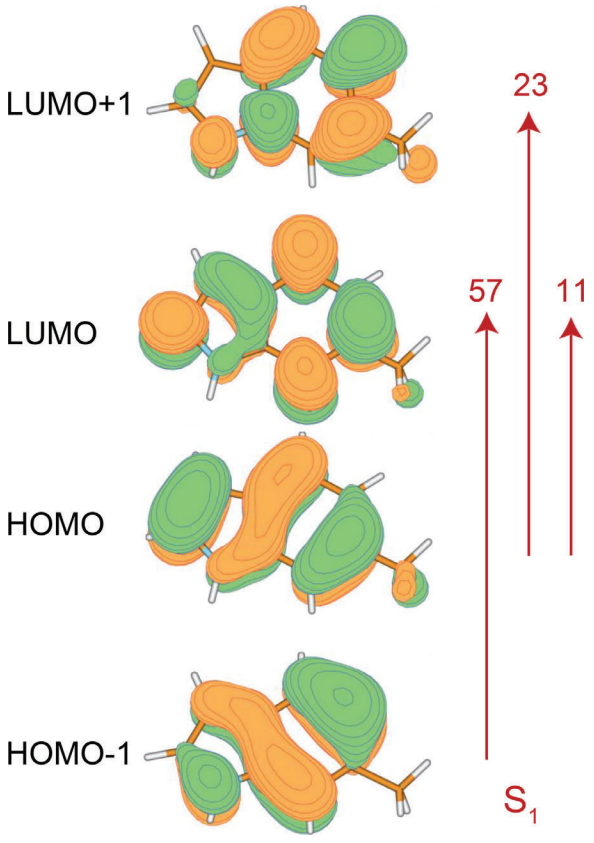

Fig. 1. Molecular orbitals of 6-methylindole with the percentage of the S_1 excitations according to SCS-CC2/cc-pVTZ calculations.

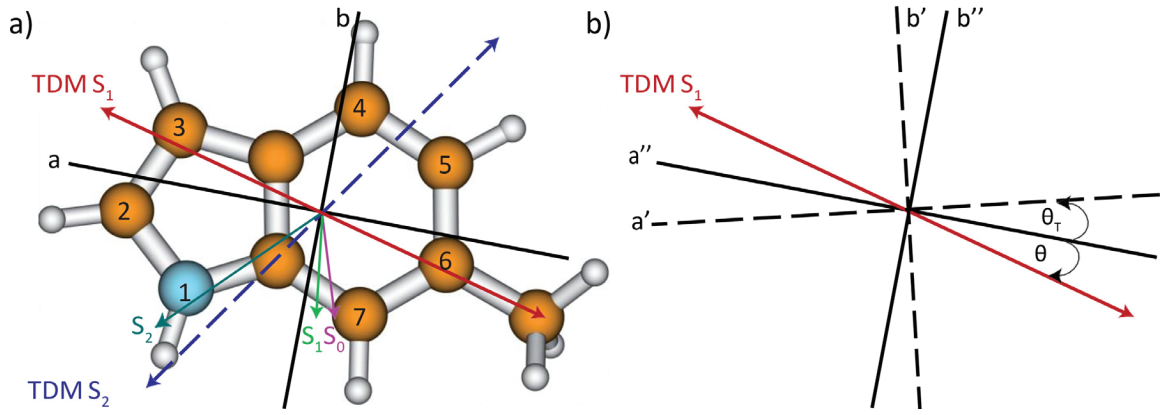

Fig. 2. (a) Optimized ground state structure, inertial axes, transition dipole moment for excitation to the lowest excited singlet state (red, straight), the orientation of the permanent dipole moment in the ground (magenta, straight), first excited state (green, straight) and second excited state (turquoise, straight) of 6-MI. The calculated transition dipole moment for the excitation to the S_2 state is shown as a blue dotted arrow. A positive sign of the angle θ and θ_D refer to a clockwise rotation of the inertial a-axis onto the dipole/TDM vector.
(b) Definitions of the axis reorientation angle θ_T and the angle of the transition dipole moment θ with the inertial a-axis. The doubly primed axes refer to the ground state, the singly primed to the electronically excited state. A negative sign of θ_T refers to a counterclockwise rotation of the inertial axis system upon electronic excitation.

Table 1
SCS-CC2/cc-pVTZ computed and experimental molecular parameters of 6-MI. Doubly primed parameters belong to the electronic ground and single primed to the excited state. θ_D is the angle of the permanent dipole moment vector with the main inertial a-axis. A positive sign of this angle means a clockwise rotation of the main inertial a-axis onto the dipole moment vector, shown in Fig. 2. θ is the angle of the transition dipole moment vector with the main inertial a-axis. The same convention for its sign is used as for θ_D. For details see text.

	Theory SCS-CC2			Experiment
	S_0	L_b	L_a	
A'' /MHz	3417.0	-	-	3428.83(9)
B'' /MHz	1040.6	-	-	1042.09(2)
C'' /MHz	801.6	-	-	802.62(2)
$\Delta I''$ / amu Å^2	−3.12	-	-	-2.70
μ''_a / D	+0.63	-	-	±0.34
μ''_b / D	−1.92	-	-	±1.81
μ''_c / D	0.00	-	-	0.00
μ'' / D	2.02	-	-	1.84
θ''_D / °	+71.9	-	-	±79.4
A' /MHz	-	3304.46	3311.2	3347.75(10)
B' /MHz	-	1028.62	1027.5	1036.90(3)
C' /MHz	-	788.4	788.0	792.78(3)
$\Delta I'$ / amu Å^2	-	−3.19	−3.12	−0.88
μ'_a / D	-	+0.3	−3.11	±0.19
μ'_b / D	-	−2.0	−3.38	±1.73
μ'_c / D	-	0.08	0.01	±0.09
μ' / D	-	2.01	4.56	1.74
θ'_D / °	-	+80.7	−47.7	±83.7
ΔA / MHz	-	−112.5	−105.8	−81.08
ΔB / MHz	-	−12.0	−13.1	−5.19
ΔC / MHz	-	−13.3	−13.6	−9.84
θ /°	-	+16.1	−54.4	±21.1(20)
θ_T /°	-	−0.4	-	−1.0
ν_0 /cm^{-1}	-	36,237	39,588	34819.41(2)
$\Delta_{Lorentz}$ /MHz	-	-	-	14.38(1)
τ / ns	-	-	-	11.07(2)
τ_r / ns	-	34.1	7.4	-

state as lowest excited singlet state. The calculated angle θ for the L_a-state is −54.4° . Both TDM orientations, along with the permanent dipole moments of all three states are shown in Fig. 2.

The value of the permanent dipole moment is 2.02 D in the ground state and stays nearly constant in the lowest excited singlet state at the SCS-CC2 level of theory with 2.01 D, both with larger amounts of the b-component of the dipole vector. The angle θ_D of the calculated permanent dipole moment with the inertial a-axis increases slightly from +71.9° ° to +80.7° ° upon excitation. For the

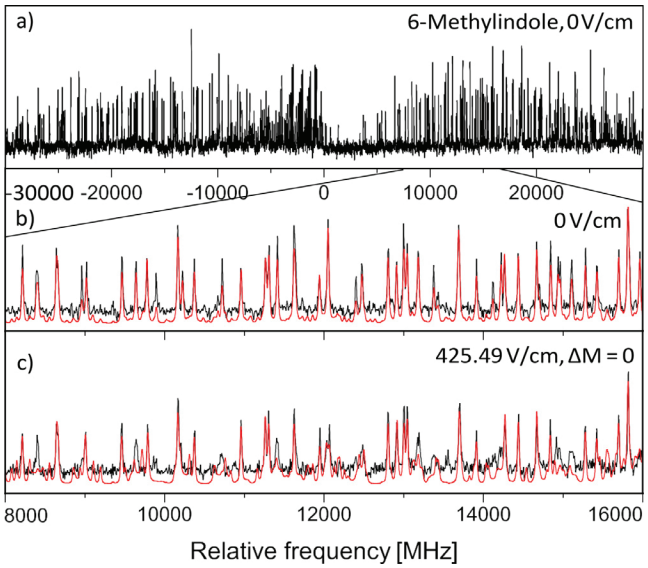

Fig. 3. Rotationally resolved electronic spectrum of the electronic origin of 6-MI, along with a simulation with the best CMA-ES fit parameters.

second excited singlet state a considerably larger dipole moment of 4.56 D is found, with an angle θ_D of −47.7° cf Fig. 2.

The pure radiative lifetime of an isolated molecule in the gas phase can be calculated by the following expression [15,41]:

$$\tau_r = \left(\frac{2\pi \cdot e^2 \cdot f}{\epsilon_0 \cdot m_e \cdot c \cdot \lambda^2} \right)^{-1} \quad (1)$$

where e is the elementary charge, f the dimensionless oscillator strength, ϵ_0 the vacuum permittivity, m_e the mass of the electron, c the speed of light, and λ the wavelength of the transition. Using Eq. (1) and the SCS-CC2/cc-pVTZ calculated oscillator strength and transition wavelength we compute a pure radiative lifetime τ_r of 34 ns for isolated 6-MI after excitation of the vibrationless origin.

4.2. Experimental results

Figure 3 shows the rotationally resolved electronic spectrum of the origin of 6-MI[1] at 34819.41(2) cm^{-1}, which is set to zero on the scale of the figure, along with the best fits using the CMA-ES algorithm at zero field (trace b) and at a field strength of 425.49 V/cm (trace c). Traces b and c cover the same spectral range. The selection rules $\Delta M = 0$ for the Stark spectrum hold, because the electric field in the chosen set-up is parallel to the polarization of the plane of the exciting light. Some lines in the zero-field spectrum are split in the electric field. Experimental spectra are shown as black traces, simulations, using the best fit parameters, as red traces with a very good agreement between both spectra. The molecular parameters from the fit using a CMA-ES algorithm are summarized in Table 1 and are compared to the results of the SCS-CC2/cc-pVTZ calculations of the S_0, S_1 (L_b) and S_2 (L_a) states.

Although the structures of 6-MI in the S_1 and S_2 states are very similar (they differ by less than 3% in *A* and by less than 1% in *B* and *C*), it is clear from the adiabatic excitation energies, and from the permanent dipole moments, that the observed state is the L_b-state. As in most cases, the dipole moment of the L_a-state is more than twice as high as for the L_b-state.

The analysis of the origin band yields an TDM angle θ of $\pm 21.1(20)^\circ$ with the inertial *a*-axis. By comparison to the *ab initio* computed value the indeterminacy of the sign of the TDM orientation can be removed. However, in the following we will show that the positive value of θ can also be deduced from experimental findings alone, without referring to the *ab initio* calculations.

The determined excited state lifetime of 11.07(2) ns was obtained from the Lorentzian linewidth of 14.38(1) MHz to the Voigt line profile using a fixed Gaussian contribution of 18.70 MHz. The Gaussian contribution was determined from a Voigt fit to a few single rovibronic lines with the boundary condition of equal Gaussian contribution to each line for 2-cyanoindole [8].

5. Discussion

5.1. Excited state structure

The inertial defect of 6-MI with a value of −2.70 amu Å^2 in the electronic ground state is more negative than in the lowest excited electronically excited state with a value of −0.88 amu Å^2. The apparent increase of planarity upon electronic excitation can be traced back to the substantially lower barrier of the methyl torsion in the excited state, rendering the methyl group more planar. Bickel *et al.* determined the ground state barrier V_3 to be 123.1 cm^{-1} and the excited state barrier to 28.2 cm^{-1} [21].

Another indication, apart from adiabatic excitation energy, dipole moment and TDM orientation for the L_b-state as lowest excited singlet state are the results of the bond lengths changes upon electronic excitation from SCS-CC2/cc-pVTZ calculations. The changes, with respect to the molecular plane and along the *a*-axis of the molecule, are quite symmetric in contrast to the much more irregular changes upon excitation to the L_a-state. The difference in the structural changes upon electronic excitation for the L_a- and the L_b-state and also for the geometry changes upon electronic excitation obtained from the SCS-CC2/cc-pVTZ optimized structure can be seen in Fig. 4. The properties of the three lowest singlet electronic states of the chromophore indole have been calculated with second-order approximate coupled-cluster theory (CC2) within the resolution-of-the-identity approximation in ref. [6].

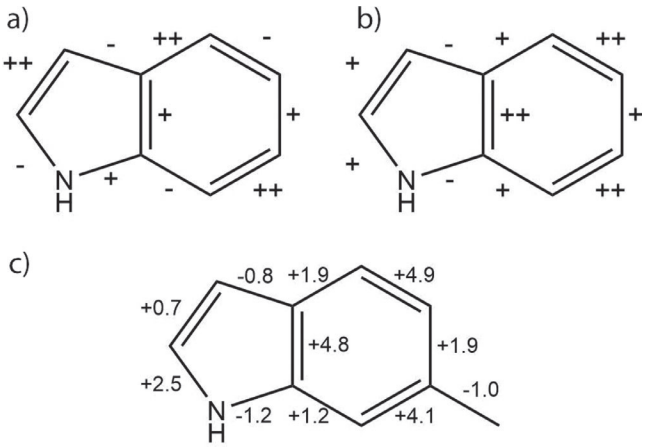

Fig. 4. Changes of the bond lengths upon electronic excitation from SCS-CC2/cc-pVTZ calculations. (a) Schematic geometry changes of the parent chromophore indole upon excitation to the L_a-state, adapted from [6]. (b) Schematic geometry changes of the parent chromophore indole upon excitation to the L_b-state, adapted from [6]. (c) Geometry changes of 6-MI in pm upon electronic excitation to the lowest excited singlet state, obtained from SCS-CC2/cc-pVTZ optimized structures. For more details see text.

5.2. Dipole moments

5.2.1. Permanent dipole moment

The experimentally determined dipole moment decreases from 1.84 D to 1.74 D upon electronic excitation. This is a clear indication, that the excited state is of L_b-character, where the permanent dipole moment normally is equal or even smaller than in the electronic ground state. The only exception, to use the change of the permanent dipole moment upon excitation of the singlet state as a sensitive indicator of the electronic nature of this excited state, was found for the molecules 2-cyanoindole and 6-methoxyindole [8,12]. Geometry changes, the TDM orientation and the orbital contributions clearly indicate the experimentally observed state as an L_b-state, but the change of the permanent dipole moment upon excitation implies an L_a-character for this excited state [8].

The angle of the permanent dipole moment with the inertial *a*-axis slightly increases from +79.4° to +83.7° upon excitation, what is less than the predicted change from +71.9° to 80.7°.

5.2.2. Transition dipole moment

The experimentally angle of the TDM, with respect to the inertial *a*-axis, was determined to be ±21.1°(20). Referring to the uncertainty of 2° the experimentally determined value is in close agreement to the theoretical value of +16.1°° at the SCS-CC2 level of theory. As it is well known, the sign of the angle θ between the TDM and the *a*-axis cannot be determined directly from the experimentally recorded spectra. The assignment of the sign of the experimentally TDM was made on the basis of the theoretical value.

Another method, to obtain the the sign of this angle, is the method of Hougen and Watson, where the wave functions of the excited state are rotated into the coordinate system of the ground state after diagonalization of the respective Hamiltonian. It is possible to determine the angle of reorientation of the inertial axis system upon electronic excitation for planar molecules θ_T [42]:

$$\tan(\theta_T) = \frac{\sum_i m_i (a_i' b_i'' - b_i' a_i'')}{\sum_i m_i (a_i' a_i'' + b_i' b_i'')} \quad (2)$$

Doubly primed coordinates refer to the principal axis system (PAS) in the electronic ground state and the singly primed coor-

[1] The observed band is the origin of the sub-torsional A component, which is due to the hindered internal rotation of the methyl group. The origin of the E sub-torsional component is shifted by 5 cm^{-1} to higher wavenumber and is therefore outside of the scanned range.

Table 2
Electronic nature of the lowest excited state, energetic shift relative to the L_b origin of indole ΔE at 35231.4 cm^{-1}, TDM orientation θ, change of dipole moment upon excitation $\Delta\mu$, and excited state life time for various substituted indoles. The TDM angles θ are given with respect to the *a*-axis of indole for better comparison and have been determined experimentally under jet-cooled conditions.

Molecule	L_a	L_b	$\Delta E/cm^{-1}$	$\theta/^\circ$	$\Delta\mu$/D	τ/ns		Ref.
Indole		✓	0	+39	−0.1	17.6	-	[4–7,43]
1-Methylindole		✓	-693.4	-	-	17.7	+I	[9,20,44]
2-Methylindole	-	-	-	-	-	15.5	+I	[44]
3-Methylindole		✓	-356.6	+46	-	13.8	+I	[4,19,20,45]
4-Methylindole	-	-	-	-	-	16.2	+I	[44]
5-Methylindole		✓	-875.5	+37	-	15	+I	[19,20]
6-Methylindole		✓	-412.0	+32	−0.10	11.1	+I	[this work]
7-Methylindole	-	-	-	-	-	15.0	+I	[44]
2,3-Dimethylindole	✓		-	-	+0.5	6	+I	[46–48]
4-Fluoroindole		✓	+410.0	+87	−0.42	6.0	-I, +M	[13]
5-Fluoroindole		✓	-895.5	±47	−0.30	12	-I, +M	[13]
6-Fluoroindole	✓	(✓)	-	−12	+0.87	6.4	-I, +M	[13]
anti-4-Methoxyindole	✓		-	−62	−0.74	3.0	+M	[12]
anti-5-Methoxyindole		✓	-2110.9	+32	−0.45	6.7	+M	[12,49]
anti-6-Methoxyindole		✓	-1514.8	+44	-	4.3	+M	[12,50]
syn-6-Methoxyindole		✓	-1283.3	+58	+0.57	4.5	+M	[12,50]
2-Cyanoindole		✓	-1808.8	+43	+1.50	9.4	-I, -M	[8]
3-Cyanoindole		✓	+68.0	+51	−0.50	9.8	-I, -M	[11]
4-Cyanoindole	✓		-	−28	+3.03	11.0	-I, -M	[15]
5-Cyanoindole	✓		-	−20	+1.03	12	-I, -M	[16]
syn-5-Hydroxyindole		✓	-2558.3	+50	-	10	-I, +M	[14]
anti-5-Hydroxyindole		✓	-2327.4	+39	−0.61	7.5	-I, +M	[14,51]
s-cis-Indole-4-carboxylic acid	✓		-	−76	-	3.7	-I, -M	[52]
s-trans-Indole-4-carboxylic acid	✓		-	−82	-	6.3	-I, -M	[52]
Carbazole	✓		-	−75	-	29.4	-M	[53,54]
Oxoindole	✓		-	−58	-	16	-M	[55]

dinates to the respective excited state inertial system. m_i are the atomic masses. We obtain an axis reorientation angle θ_T of -0.4° using the PAS coordinates of SCS-CC2 optimized structures for the electronic ground and lowest excited state. Since the combination of θ negative and θ_T positive and *vice versa* had a better cost function using an axis reorientation Hamiltonian than the combination of both angles negative or positive, we know that θ and θ_T must have different signs. Given that θ_T is defined geometrically from the optimized structures in both states, the sign of θ can be determined. The absolute orientation of the TDM vector θ with the *a*-axis is +21.1°, as the inertial *a*-axis calculated in the SCS-CC2 optimized structures rotates anticlockwise upon excitation.

Relating to the results of indole the orientation of the TDM of 6-MI is clearly that of an L_b-state. In indole the orientation of the TDM vector points away from the hetero atom of the pyrrole ring, what is known from linear dichroism measurements [4] and from rotationally resolved electronic spectroscopy [5].

Table 2 gives the electronic nature (L_a or L_b), the shift of the L_b origins with respect to the L_b origin of indole at 35231.4 cm^{-1}, the TDM angle θ, the excited state lifetime τ and electronic nature of the substituent (+M = positive, electron donating mesomeric effect, -M = negative, electron withdrawing mesomeric effect, +I = positive, electron donating inductive effect, -I = negative, electron withdrawing inductive effect) for a series of differently substituted indoles. To make results comparable, the angle θ is not defined as angle between the TDM and the *a*-axis of the respective compound, but as angle between the TDM and the *a*-axis of the parent indole. This allows to compare the TDM angles of the different indole derivatives directly. Interestingly, there is no obvious connection between position of substitution, electronic effect of the substituent, excited state life lime and the electronic nature of the lowest excited singlet state.

The only correlation that exists between the nature of the excited state and an observable is the change of the permanent dipole moment upon excitation. In case that the excited state is an L_b-state, the dipole moment changes are small to moderate negative, i.e. the dipole moments in the excited states are slightly smaller than in the ground state. For the excited state being an L_a-state, the dipole moment changes are large and positive. L_a-state dipole moments are between 0.5 D (2,3-dimethylindole) and 3.03 D (4-cyanoindole) larger than the corresponding ground state moment.

The energetic shifts of the L_b origins of the substituted indoles with respect to the L_b origin of indole at 35231.4 cm^{-1} show a large range between a blue-shift of 410.0 (4-fluoroindole) and a red-shift of 2558.3 cm^{-1} cm^{-1}(syn-5-hydroxyindole). Neither substitution position, nor electronic nature of the substituent show any correlation with the energetic shift. If one compares eg. 4- and 5-fluoroindole the shift of +410.0 reverses to -895.5 cm−1,cm^{-1} although the substituent and therefore its electronic nature is the same. The same holds for a comparison of 2- and 3-cyanoindole (-1808.8 *vs.* +68.0 cm^{-1}).

6. Conclusions

The lowest electronically excited singlet state of 6-MI could be identified as an L_b-state. Referring to the experimentally determined orientation of the transition dipole moment, the absolute values of the permanent dipole moments in the ground and excited state, and the geometry changes for excitation to the lowest excited singlet state this assignment has been made. The fluorescence lifetime of isolated 6-MI in the gas phase could be determined from the Lorentz contribution to the Voigt profile of the rovibronic lines to be 11.1 ± 0.2 ns.

Declaration of Competing Interest

The authors declare that they have no known competing financial interests or personal relationships that could have appeared to influence the work reported in this paper.

CRediT authorship contribution statement

Marie-Luise Hebestreit: Investigation, Validation, Formal analysis, Writing – original draft, Writing – review & editing, Visualiza-

tion. **Hajo Böschen:** Investigation, Formal analysis. **Hilda Lartian:** Investigation. **W. Leo Meerts:** Methodology, Software. **Michael Schmitt:** Conceptualization, Methodology, Software, Supervision, Funding acquisition, Writing – original draft, Writing – review & editing.

Acknowledgements

Financial support of the Deutsche Forschungsgemeinschaft *via* grant SCHM1043/14-1 is gratefully acknowledged. Computational support and infrastructure was provided by the "Center for Information and Media Technology" (ZIM) at the Heinrich-Heine-University Düsseldorf (Germany).

Supplementary material

Supplementary material associated with this article can be found, in the online version, at doi:10.1016/j.molstruc.2021.132053.

References

[1] J.R. Platt, Classification of spectra of cata-condensed hydrocarbons, J. Chem. Phys. 17 (1949) 484–495.
[2] G. Weber, Fluorescence-polarization spectrum and electronic-energy transfer in tyrosine, tryptophan and related compounds, Biochem. J. 75 (1960) 335–345.
[3] P.R. Callis, Molecular orbital theory of the ^1L_b and ^1L_a states of indole, J. Chem. Phys. 95 (1991) 4230.
[4] B. Albinsson, B. Nordén, Excited-state properties of the indole chromophore – electronic-transition moment directions from linear dichroism measurements – effect of methyl and methoxy substituents, J. Phys. Chem. 96 (1992) 6204.
[5] G. Berden, W.L. Meerts, E. Jalviste, Rotationally resolved ultraviolet spectroscopy of indole, indazole and benzimidazole: inertial axis reorientation in the $S_1(^1L_b) \leftarrow s_0$ transition, J. Chem. Phys. 103 (1995) 9596–9606.
[6] C. Brand, J. Küpper, D.W. Pratt, W.L. Meerts, D. Krügler, J. Tatchen, M. Schmitt, Vibronic coupling in indole: I. Theoretical description of ^1l_a and ^1l_b interactions and the absorption spectrum, Phys. Chem. Chem. Phys. 12 (2010) 4968–4997.
[7] J. Küpper, D.W. Pratt, W.L. Meerts, C. Brand, J. Tatchen, M. Schmitt, Vibronic coupling in indole: II. Investigation of the $^1L_a - {}^1L_b$ interaction using rotationally resolved electronic spectroscopy, Phys. Chem. Chem. Phys. 12 (2010) 4980–4988.
[8] M.-L. Hebestreit, H. Lartian, C. Henrichs, R. Kühnemuth, W.L. Meerts, M. Schmitt, Excited state dipole moments and lifetimes of 2-cyanoindole from rotationally resolved electronic Stark spectroscopy, Phys. Chem. Chem. Phys. 23 (2021) 10196–10204.
[9] M.M. Lindic, M. Schmitt, Ground and excited state dipole moments of 1-methylindole from thermochromic shifts in absorption and emission spectra, J. Photochem. Photobiol. A 406 (2021) 112984.
[10] M.-L. Hebestreit, H. Lartian, M. Schneider, R. Kühnemuth, A.Y. Torres-Boy, S. Romero-Servin, J.A. Ruiz-Santoyo, L. Alvarez-Valtierra, W.L. Meerts, M. Schmitt, Structure and excited state dipole moments of oxygen containing heteroaromatics: 2,3-benzofuran, J. Mol. Struct. 1210 (2020) 127992.
[11] M. Schneider, M.-L. Hebestreit, M.M. Lindic, H. Parsian, A.Y. Torres-Boy, L. Álvarez Valtierra, L. Meerts, R. Kühnemuth, M. Schmitt, Rotationally resolved electronic spectroscopy of 3-cyanoindole and the 3-cyanoindole-water complex, Phys. Chem. Chem. Phys. 20 (2018) 23441–23452.
[12] M. Wilke, J. Wilke, C. Brand, M. Schmitt, Influence of the position of the methoxy group on the stabilities of the syn and anti conformers of 4-, 5-, and 6-methoxyindole, J. Mol. Spect. 337 (2017) 137–144.
[13] J. Wilke, M. Wilke, C. Brand, J.D. Spiegel, a.S. Christel M. Marian, Modulation of the La/Lb mixing in an indole derivative: a position-dependent study using 4, 5, and 6-fluoroindole, J. Phys. Chem. A 121 (2017) 1597–1606.
[14] O. Oeltermann, C. Brand, M. Wilke, M. Schmitt, Ground and electronically excited singlet state structures of the syn and anti rotamers of 5-hydroxyindole, J. Phys. Chem. A 116 (2012) 7873–7879.
[15] M.-L. Hebestreit, M. Schneider, H. Lartian, V. Betz, M. Heinrich, M. Lindic, M.Y. Choi, M. Schmitt, Structures, dipole moments and excited state lifetime of isolated 4-cyanoindole in its ground and lowest electronically excited singlet states, Phys. Chem. Chem. Phys. 21 (2019) 14766–14774.
[16] O. Oeltermann, C. Brand, B. Engels, J. Tatchen, M. Schmitt, The structure of 5-cyanoindole in the ground and lowest electronically excited singlet state, deduced from rotationally resolved electronic spectroscopy and ab initio theory, Phys. Chem. Chem. Phys. 14 (2012) 10266–10270.
[17] O. Oeltermann, C. Brand, W.L. Meerts, J. Tatchen, M. Schmitt, Rotationally resolved electronic spectroscopy of 2,3-bridged indole derivatives: tetrahydrocarbazole, J. Mol. Struct. 933 (2011) 2–8.
[18] A.L. Sobolewski, W. Domcke, Ab initio investigations on the photophysics of indole, Chem. Phys. Lett. 315 (1999) 293–298.
[19] K. Remmers, E. Jalviste, I. Mistrík, G. Berden, W.L. Meerts, Internal rotation effects in the rotationally resolved $S_1^1L_b \leftarrow s_0$ origin bands of 3-methylindole and 5-methylindole, J. Chem. Phys. 108 (1998) 8436–8445.
[20] T.M. Korter, D.W. Pratt, Perturbations of the fully resolved electronic spectra of large molecules by the internal rotation of attached methyl groups. influence of complex formation, J. Phys. Chem. B 105 (2001) 4010–4017.
[21] G.A. Bickel, G.W. Leach, D.R. Demmer, J.W. Hager, S.C. Wallace, The torsional spectra of jet-cooled substituted indoles in the ground and first excited states, J. Chem. Phys. 88 (1988) 1–8.
[22] R. Ahlrichs, M. Bär, M. Häser, H. Horn, C. Kölmel, Electronic structure calculations on workstation computers: the program system turbomole, Chem. Phys. Lett. 162 (1989) 165–169.
[23] J. T. H. Dunning, Gaussian basis sets for use in correlated molecular calculations. I. The atoms boron through neon and hydrogen, J. Chem. Phys. 90 (1989) 1007–1023.
[24] C. Hättig, F. Weigend, Cc2 excitation energy calculations on large molecules using the resolution of the identity approximation, J. Chem. Phys. 113 (2000) 5154–5161.
[25] C. Hättig, A. Köhn, Transition moments and excited-state first-order properties in the coupled cluster model CC2 using the resolution-of-the-identity approximation, J. Chem. Phys. 117 (2002) 6939–6951.
[26] C. Hättig, Geometry optimizations with the coupled-cluster model CC2 using the resolution-of-the-identity approximation, J. Chem. Phys. 118 (2002) 7751–7761.
[27] A. Hellweg, S. Grün, C. Hättig, Benchmarking the performance of spin-component scaled CC2 in ground and electronically excited states, Phys. Chem. Chem. Phys. 10 (2008) 1159–1169.
[28] P. Deglmann, F. Furche, R. Ahlrichs, An efficient implementation of second analytical derivatives for density functional methods, Chem. Phys. Lett. 362 (2002) 511–518.
[29] W.L. Meerts, M. Schmitt, G. Groenenboom, New applications of the genetic algorithm for the interpretation of high resolution spectra, Can. J. Chem. 82 (2004) 804–819.
[30] W.L. Meerts, M. Schmitt, A new automated assign and analyzing method for high resolution rotational resolved spectra using genetic algorithms, Phys. Scripta 73 (2005) C47–C52.
[31] W.L. Meerts, M. Schmitt, Application of genetic algorithms in automated assignments of high-resolution spectra, Int. Rev. Phys. Chem. 25 (2006) 353–406.
[32] M. Schmitt, W.L. Meerts, Rotationally resolved electronic spectroscopy and automatic assignment techniques using evolutionary algorithms, in: M. Quack, F. Merkt (Eds.), Handbook of High Resolution Spectroscopy, John Wiley and Sons, 2011. ISBN: 978-0-470-06653-9
[33] A. Ostermeier, A. Gawelcyk, N. Hansen, Step-size adaptation based on non-local use of selection information, in: Y. Davidor, H.-P. Schwefel, R. Männer (Eds.), Parallel Problem Solving from Nature, PPSN III, Springer, Berlin/Heidelberg, 1994.
[34] N. Hansen, A. Ostermeier, Completely derandomized self-adaptation in evolution strategies, Evol. Comput. 9 (2) (2001) 159–195.
[35] W. Gordy, R.L. Cook, Microwave Molecular Spectra, third ed., Wiley, New York, 1984.
[36] S. Gerstenkorn, P. Luc, Atlas du Spectre d'Absorption de la Molécule d'iode 14800–20000 cm^{-1}, CNRS, Paris, 1986.
[37] M. Schmitt, Spektroskopische Untersuchungen an Wasserstoffbrückenbindungen, Heinrich-Heine-Universität, Math. Nat. Fakultät, Düsseldorf, 2000 Habilitation.
[38] M. Schmitt, J. Küpper, D. Spangenberg, A. Westphal, Determination of the structures and barriers to hindered internal rotation of the phenol-methanol cluster in the S_0 and S_1 state, Chem. Phys. 254 (2000) 349–361.
[39] J. Wilke, M. Wilke, W.L. Meerts, M. Schmitt, Determination of ground and excited state dipole moments via electronic stark spectroscopy: 5-methoxyindole, J. Chem. Phys. 144 (2016) 044201–1–044201–10.
[40] K. Wohlfart, M. Schnell, J.U. Grabow, J. Küpper, Precise dipole moment and quadrupole coupling constants of benzonitrile, J. Mol. Spec. 247 (2014) 119–121.
[41] R.S. Friedman, P.W. Atkins, Molecular Quantum Mechanics, Oxford University Press, New York, 2011.
[42] J.T. Hougen, J.K.G. Watson, Anomalous rotational line intensities in electronic transitions of polyatomic molecules: axis-switching, Can. J. Phys. 43 (1965) 298–320.
[43] C. Kang, T.M. Korter, D.W. Pratt, Experimental measurement of the induced dipole moment of an isolated molecule in its ground and electronically excited states: indole and indole-h_2o, J. Chem. Phys. 122 (2005) 174301.
[44] Y. Huang, M. Sulkes, Anomalously short fluorescence lifetimes in jet cooled 4-hydroxyindole. evidence for excited state tautomerism and proton transfer in clusters, Chem. Phys. Lett. 254 (1996) 242–248.
[45] S. Arnold, M. Sulkes, Spectroscopy of Solvent Complexes with Indoles: Induction of ^1L_a-^1L_b State Coupling, J. Phys. Chem. 96 (1992) 4768.
[46] K.W. Short, P.R. Callis, One- and two-photon spectra of jet-cooled 2,3-dimethylindole: ^1L_b and ^1L_a assignments, Chem. Phys. 283 (2002) 269.
[47] D.R. Demmer, G.W. Leach, E.A. Outhouse, J.W. Hager, S.C. Wallace, Excited-State Dynamics of Jet-Cooled Substituted Indoles: The Role of Polar Interactions in L_a - L_b State Coupling, J. Phys. Chem. 94 (1990) 582.
[48] I. Gryczyski, A. Kawski, Temperaturabhängigkeit der statischen dielektrizitätskonstante und des optischen brechungsindexes von flüssigkeiten, Z. Naturforsch. 30A (1975) 287–291.

[49] C. Brand, O. Oeltermann, D.W. Pratt, R. Weinkauf, W.L. Meerts, W. van der Zande, K. Kleinermanns, M. Schmitt, Rotationally resolved electronic spectroscopy of 5-methoxyindole, J. Chem. Phys. 133 (2010) 024303–1–024303–11.
[50] C. Brand, O. Oeltermann, M. Wilke, M. Schmitt, Position matters: high resolution spectroscopy on 6-methoxyindole, J. Chem. Phys. 138 (2013) 024321.
[51] J. Wilke, M. Wilke, C. Brand, W.L. Meerts, M. Schmitt, On the additivity of molecular fragment dipole moments of 5-substituted indole derivatives, Chemphyschem 17 (17) (2016) 2736–2743.
[52] J.T. Yi, S. Romero-Servin, L. Álvarez Valtierra, D.F. Plusquellic, Rotationally resolved uv spectroscopy of the rotamers of indole-4-carboxylic acid: evidence for charge transfer quenching, J. Chem. Phys. 152 (2020) 144307.
[53] J.T. Yi, L. Álvarez Valtierra, D.F. Plusquellic, Rotationally resolved S_1- S_0 electronic spectra of fluorene, carbazole, and dibenzofuran: Evidence for Herzberg-Teller coupling with the S_2 state, J. Chem. Phys. 124 (2006) 244302.
[54] A.R. Auty, A.C. Jones, D. Phillips, Time-resolved fluorescence of jet-cooled carbazoles and their weak complexes, J. Chem. Soc. Faraday Trans. 2 82 (1986) 1219.
[55] J.A. Minguela-Gallardo, J.T. Yi, D.F. Plusquellic, L. Álvarez Valtierra, Rotationally resolved electronic s1 spectra of tryptoline and oxindole: reversal of the 1La and 1Lb state character, J. Mol. Struct. (2021). accepted for publication